*AAPS PharmSciTech, Vol. 14, No. 1, March 2013 (© 2012)*
DOI: 10.1208/s12249-012-9894-0

*Research Article*

# Design, Characterization, and *In Vitro* Evaluation of Antifungal Polymeric Films

**Daniel A. Real,[1] María V. Martinez,[1] Agustín Frattini,[2] Marina Soazo,[3] Alicia G. Luque,[4] Marisa S. Biasoli,[4] Claudio J. Salomon,[1,3] Alejandro C. Olivieri,[3,5] and Darío Leonardi[1,3,6]**

*Received 14 August 2012; accepted 9 November 2012; published online 8 December 2012*

***Abstract.*** The objective of the present paper was the development and the full characterization of antifungal films. Econazole nitrate (ECN) was loaded in a polymeric matrix formed by chitosan (CH) and carbopol 971NF (CB). Polyethylene glycol 400 and sorbitol were used as plasticizing agents. The mechanical properties of films were poorer when the drug was loaded, probably because crystals of ENC produces network outages and therefore reduces the polymeric interactions between the polymers. Polymers–ECN and CH–CB interactions were analyzed by Fourier-transform infrared spectroscopy (FTIR), thermal gravimetry analysis, and differential thermal analysis (DTA-TGA). ECN did not show structure alterations when loaded into the films. In scanning electron microphotographs and atomic force microscopy analysis, films prepared with CB showed an evident wrinkle pattern probably due to the strong interactions between the polymers, which were observed by FTIR and DTA-TGA. The *in vitro* activity of the formulations against *Candida krusei* and *Candida parapsilosis* was twice as greater as the commercial cream, probably as a result of the antifungal combination of the drug with the CH activity. All these results suggest that these polymeric films containing ECN are potential candidates in view of alternatives dosages forms for the treatment of the yeast assayed.

**KEY WORDS:** anti-fungal activity; drug delivery systems; *in vitro* models; infrared spectroscopy; thermogravimetric analysis.

## INTRODUCTION

Chitosan (CH), a cationic biocompatible and biodegradable biopolymer used for biomedical applications is a polysaccharide derived from chitin (1). This polymer obtained mainly by extraction from crustacean shells such as crab and shrimp, has been used in diverse fields, such as seed coating, as fuel cell membranes, controlled drug delivery systems, membrane-based transdermal drug delivery systems, wound healing, dressing material, and tissue engineering (1–5). Depending on its application, CH can be formulated as microparticles or nanoparticles, powders, hydrogels, or films (6–8). Specifically, films based on CH have been mainly developed for food packaging (9), or for pharmaceutical applications. In the latter case, different administration routes and uses such as buccal delivery of flufenamic (10), control release of amoxicillin in stomach for the treatment of *Helicobacter pylori* (11), vaginal delivery of metronidazole for the treatment of bacterial vaginosis (12), or potential skin drug delivery systems (13) were evaluated. Several works have studied the mechanical properties of CH films, demonstrating that these properties may be improved when CH forms polyelectrolyte complexes with other polymers oppositely charged (14,15). Carbopol 971NF (CB) is a useful polymer which may be anionic, depending on the pH value, and therefore it may generate ionic interactions with CH. This polymer is frequently employed as a major component of drug delivery gel systems for buccal, transdermic, ocular, rectal, and nasal applications (16). Thus, the interaction between the polymers may produce a polymeric matrix which could be able to transport and release different drugs. Antifungal agents are interesting drugs to be used as model due to, among the different microbes that affect the quality of life of the entire population, infectious diseases caused by human pathogenic fungi represent a major and global health problem (17). Aside from fungi, the opportunistic yeasts are acquiring major importance due to the increase of extremely aged persons, patients in intensive care units, and the use of antibiotics and immunosuppressive agents (18). Additionally, the advances in medical management as antineoplasic chemotherapy, organ transplantation, parenteral nutrition, invasive surgical procedures, and the human immunodeficiency virus infection, allowed a continuous

[1] Departamento de Tecnología Farmacéutica, Universidad Nacional de Rosario, Suipacha 531, Rosario 2000, Argentina.
[2] Departamento de Física, Facultad de Ciencias Bioquímicas y Farmacéuticas, Universidad Nacional de Rosario (UNR), Suipacha 531, Rosario 2000, Argentina.
[3] Instituto de Química Rosario (IQUIR, UNR-CONICET), Suipacha 531, Rosario 2000, Argentina.
[4] Centro de Referencia de Micología, (CEREMIC) Facultad de Ciencias Bioquímicas y Farmacéuticas, UNR, Suipacha 531, Rosario 2000, Argentina.
[5] Departamento de Química Analítica, Facultad de Ciencias Bioquímicas y Farmacéuticas, UNR, Suipacha 531, Rosario 2000, Argentina.
[6] To whom correspondence should be addressed. (e-mail: dleonard@fbioyf.unr.edu.ar)

growth of *Candida*-associated diseases (19,20). Among them, *Candida parapsilopsis* is able to cause infections of the human skin, the mucosa, and the viscera, while the less virulent *Candida krusei* causes nosocomial infections (21). On the other hand, vaginal yeast infections are one of the most common reasons of women seeking healthcare, and it has been estimated that 70–75% of women will have an episode of *Candida vaginitis* at least once during their lifetime (22). Several drugs are used to treat these pathologies, between them, econazole nitrate (ECN), an imidazole antifungal agent, is mostly administered topically for the treatment of skin infections and vaginal candidiasis (23). Particularly, vaginal delivery is an important route of drug administration for both local and systemic diseases. The vaginal route appears to be highly appropriate for bioadhesive drug delivery systems in order to retain drugs for treating largely local conditions (24). Consequently, and due to the reported mucoadhesive properties of both CH and CB (25–27), the development of films based on these polymers and loaded with ECN may be adequate for a potential vaginal administration. Therefore, the aims of the present work were: (1) to develop polymeric films loaded with ECN as model drug, (2) to evaluate their mechanical properties, interactions between the components and microscopic morphology, and (3) to investigate if the matrix is able to release the drug and compare the *in vitro* antifungal activity of the films *versus* an antifungal commercial cream.

## MATERIALS AND METHODS

### Materials

Chitosan (230 KDa average molecular weight and 80.6% of *N*-deacetylation) was supplied by Aldrich Chemical Co. (Milwaukee, WI, USA), carbomer (Carbopol ® 971NF) by Lubrizol Advanced Materials, Inc. (Cleveland, OH, USA), and econazole nitrate pharmaceutical grade, by Parafarm, (Buenos Aires, Argentina). All other chemicals were of analytical grade.

### Methods

#### *Preparation of the Films*

Chitosan solutions (1% *w*/*v*) were prepared by dispersing CH in aqueous lactic acid solution (2% *v*/*v*) and stirring overnight (28). CB solutions (1% *w*/*v*) were prepared by dissolving in water. The pH of the solutions was adjusted at 1 by addition of 1 M HCl, in order to avoid precipitation when mixing the solutions of the polymers (13,29). Both CH and CB solutions were filtered through Miracloth® (Calbiochem-Novabiochem Corp., San Diego, CA) to remove impurities prior to use. The CH solutions were dripped to the CB solutions and mixed with a mechanical stirrer during 5 min. Then sorbitol (S) or polyethyleneglycol 400 (PEG 400) 20% and ECN powder at 1% *w*/*w* (previously blended through a 10-μm filter) were added (Table I summarizes the films compositions, working conditions, and the coding used). The mixture was stirred at 200 rpm during 2 h in a magnetic Boecco stirrer (Germany). The solutions were then cast on Petri dishes (10 cm in diameter) and dried in an oven at 25°C, constant RH (58%). After drying, films were neutralized in casting by addition of NaOH solution 5% (*w*/*v*), washed with distilled water, and dried again (30,31). Dried films were removed from the plates and conditioned in a chamber (25°C and 58% RH) for 3 days. The films used in the different tests were selected based on the lack of physical defects such as cracks, bubbles, and holes.

**Table I.** Summarizes the Films Compositions, Working Conditions, and the Coding Used in What Follows

| Formulation | CH (%) | CB (%) | PEG 400 (%) | S (%) | ECN (% *w*/*w*) |
|---|---|---|---|---|---|
| FI | 100 | 0 | 2 | – | 0 |
| FII | 100 | 0 | 2 | – | 1 |
| FIII | 100 | 0 | – | 2 | 0 |
| FIV | 100 | 0 | – | 2 | 1 |
| FV | 90 | 10 | 2 | – | 0 |
| FVI | 90 | 10 | 2 | – | 1 |
| FVII | 90 | 10 | – | 2 | 0 |
| FVIII | 90 | 10 | – | 2 | 1 |
| FIX | 80 | 20 | 2 | – | 0 |
| FX | 80 | 20 | 2 | – | 1 |
| FXI | 80 | 20 | – | 2 | 0 |
| FXII | 80 | 20 | – | 2 | 1 |

#### *Film Thickness*

Film thickness was measured with a digital micrometer (Schwyz, China). For each film, ten thickness measurements were made. Averaged values of thickness measurements were calculated and used in all calculations.

#### *Mechanical Properties*

Mechanical strengths of the films were evaluated using a Universal Testing Machine Instron, single column, Series 3340 (Instron, Norwood, MA, United States) with a 10-N load cell. Eight replicate measurements were performed by each mechanical test. Probes for each mechanical test were conditioned for 1 day at 25°C and 58% RH and equilibrated to the testing environment for 2 h at 22°C and 50% RH on average. In the puncture test, films (90 mm diameter) were fixed to a support with a circular opening, and a cylindrical probe (2 mm diameter) was moved perpendicularly to the film surface at a constant speed (0.8 mm/s) until the probe passed through the film. Force–deformation curves were obtained. Force (Newtons) and deformation (millimeters) values at the puncture point were then recorded to represent the puncture strength (PS) and deformation (D) of the films (32). To evaluate tensile properties, films were cut into strips (7 mm wide and 60 mm length) using a scalpel. The strip ends were mounted with double-sided tape and squares of 30 mm of cardstock (to prevent tearing and slippage in the testing device) (33). Between cardstock ends, the exposed film strip length was 30 mm. The initial grip distance was 30 mm and the crosshead speed was 0.05 mm/s. The parameters obtained from stress–strain curves were: tensile strength (TS), calculated by dividing the peak load by the cross-sectional area (thickness of film) of the initial film, and elongation (E), calculated as the percentile of the change in the length of specimen respect to the original distance between the grips (30 mm).

*Fourier Transform Infrared Spectroscopy*

Fourier transform infrared (FT-IR) spectra were obtained by an FT-IR-Prestige-21 (Shimadzu, Tokyo, Japan) using the KBr disk method (2 mg sample in 100 mg KBr). Scanning range was 450 to 3,900 $cm^{-1}$ with a resolution of 1 $cm^{-1}$.

*Thermal Gravimetric Analysis and Differential Thermal Analysis*

The films, the polymers, and ECN were investigated by thermal gravimetry analysis and differential thermal analysis (TGA-DTA) methods, using equipment having a high sensitive weight balance (Shimadzu DTG60). Samples of approximately 20 mg, consisting in drug, polymers powder, or pieces of films, were heated at a rate of 10°C/min up to 700°C. All curves were normalized to unity of the initial sample mass.

*Scanning Electron Microscopy*

The morphology of the films was investigated by scanning electron microscopy (SEM) using an AMR 1000 Scanning Microscope (Amray, Bedford, MA). Films were mounted on an aluminum sample support by means of a conductive and double-sided adhesive. Samples were previously sputter coated with a gold layer in order to make them conductive.

*Atomic Force Microscopy*

Atomic force microscopy (AFM) images were obtained using a NanoTec Electronica AFM equipment. All images were obtained on contact mode and at a scan rate of 2 Hz. The 3D surfaces and rugosity distribution were analyzed employing WSxM 4.0 betha 5.0 software (34).

*Water Uptake.* In order to obtain a full characterization of the matrix, the affinity of the systems by water was determined. Each film was soaked in 200 ml of citrate buffer pH 4.2 or phosphate buffer pH 7.2 at 37°C. To estimate the amount of water absorbed at different times, the systems were taken out, carefully wiping off excess of medium and quickly weighed, then the samples were placed back in water.

The water uptake percentage was calculated according to the following equation:

$$\text{Water uptake} = (\text{Fs}-\text{Fd})/\text{Fd} \times 100\%,$$

where Fs = mass of the swollen film and Fd = mass of the dry film.

*Dissolution Studies*

Dissolution studies of ECN from the matrices were performed in 900 ml of either in citrate buffer (pH 4.2) or in phosphate buffer (pH 7.2) at 37°C, using a USP XXIV apparatus (Hanson Research, SR8 8-Flask Bath, Ontario, Canada) with paddle rotating at 50 rpm. At different time intervals, 5 ml samples were withdrawn through a filter. The amount of released ECN was determined by UV analysis at 270 nm. It was found that the excipients did not interfere with the assay at this wavelength. The results presented are mean values of three determinations.

*Halo Zone Test*

Halo zone test was used to analyze the release of the antifungal agent contained in the samples. A film of CH 100% without drug and commercial cream (CC) containing the same concentration of ECN were used as controls. CC (1% ECN and excipients: stearic acid, cetilic alcohol, triethanolamine, PEG 400, sorbitol, and propylparben) was lean on a 5-mm round aluminum disk which was used as support of the cream. The *in vitro* activity of the films were evaluated by the diffusion method in an agar Müeller Hinton medium, using *C. krusei* (ATCC 6258) and *Candida parapsilosis* (ATCC 22019) as yeast for the tests. The films were taken, cut into 5 mm round films, and leaned (with the controls) in Petri dishes that were incubated at 37°C. The anti-fungal activity of the films on the plate was determined according to the size of the inhibitory zone at a fixed time. The assay was developed by triplicate (35).

*Stability Study*

Representative samples were placed in a controlled temperature cabinet at 25°C or 40°C and 58% RH (36). Monthly, films were dissolved by magnetic stirred in citrate buffer, 900 ml (pH 4.2) for 48 h at 37°C, then the solutions were filtered through 0.20-μm membrane filter. The amount of ECN release was analyzed by UV at 270 nm.

*Statistical Analysis*

Results are expressed as mean ± standard error. Analysis of variance was used and when the effect of the factors was significant ($p<0.05$), the Tukey multiple ranks honestly significant difference test was applied (95% of confidence level).

## RESULTS AND DISCUSSION

### ECN Films Characterization

*Mechanical Properties*

As can be observed in Fig. 1, the thickness of the films was not affected by the parameters analyzed, not showing significant differences between the formulations even when the films were loaded with ECN ($p>0.05$). In the formulations without drug, the effect of sorbitol (S) was evident over PS, deformation, TS, and E, producing more elastic and flexible films, with better mechanical properties than those containing PEG 400 in the matrix. This is probably because S could act by the same mechanism of glycerol as internal plasticizer, penetrating through the polymer matrix and interfering with CH chains, decreasing intermolecular attraction and increasing polymer mobility, which led films to be more flexible. In contrast, PEG 400 acts as an external plasticizer (37) producing films with poor mechanical properties. This fact could be explained due to the fact that crystalline structures of polymeric materials are stabilized by second-order bonds, which are destroyed by plasticizers, modifying the

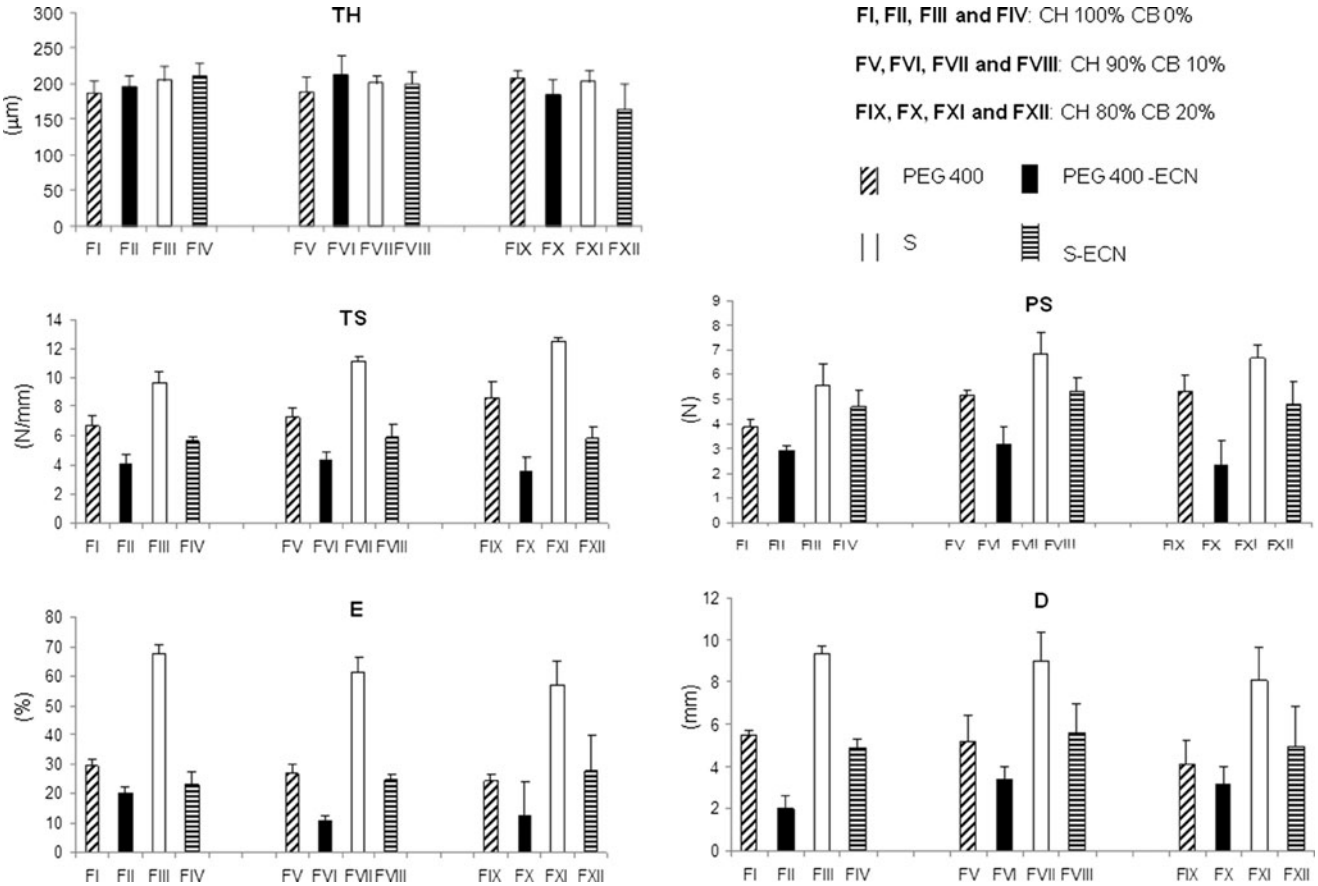


**Fig. 1.** Thickness (*TH*) of the films and parameters calculated from stress–strain (*TS* and *E*) and force-deformation curves (*PS* and *D*)

mechanical properties of materials without altering their fundamental chemical character. During external plasticization, only weak second-order bonds develop between the plasticizer and the polymer, while internal plasticizers are covalently bound to the plasticized material. External plasticizers can migrate in the polymer, which may lead to recrystallization of the material and loss of elasticity (37).

The addition of ECN significantly decreased all the parameters evaluated in tensile and puncture tests ($p<0.05$), while no trend could be observed in relation with CB concentration. These results could be attributed to the disruption of the homo and hetero-polymeric interactions which are the matrix former and the responsible of the mechanical properties. Such disruption of the matrix probably induces the development of a heterogeneous film structure, resulting in a decrease in both tensile strength and elongation. The measurement of the mechanical properties of edible films is important because they are related to their durability, as well as to the ability to resist the manipulation when they are applied over zones affected by the pathology. Due to the fact that the films with better mechanical properties (even when ECN was loaded) were obtained employing S, the formulations containing this plasticizer were selected for further assays.

*Fourier Transform Infrared Spectroscopy*

FTIR spectra of pure ECN, CB, and CH powders and of films FXI and FXII (20% CB with and without ECN) are shown in Fig. 2. The characteristic bands of pure ENC are observed at 1,585, 1,548, 828, 804, and 638 $cm^{-1}$ (38). The CH spectrum showed a broad band with a maximum at 3,440 $cm^{-1}$, assigned to the stretching vibration of O–H and N–H groups associated by intra- and intermolecular hydrogen bonding. Absorption at 1,656 $cm^{-1}$ (C=O stretching) and 1,599 $cm^{-1}$ (N–H stretching) are characteristic of amide groups. Finally, the broad band absorption at 1,090 $cm^{-1}$ is assigned to the overlapping of the bands at 1,049, 1,057, and 988 $cm^{-1}$ assigned to CHs saccharide structure (39). In the CB spectrum, formation of intramolecular hydrogen bonding can be characterized by a broad band at 3,218 $cm^{-1}$. The absorption band at 1,708 $cm^{-1}$ has been assigned to C=O stretching vibration from carboxylic groups. The presence of bands in the range of 1,500–1,150 $cm^{-1}$ has been assigned to C–O–C stretching vibrations. The films spectra were similar to the CH spectrum, as expected, considering that the CH/CB ratio used were 90:10 (data not shown) and 80:20, without and with 1% of ECN (formulations FXI and FXII, respectively).

However, the peak at 1,599 $cm^{-1}$ assigned to the amine band of chitosan was shifted to 1,640 $cm^{-1}$, indicating that the $NH_2$ group was protonated to a $NH_3^+$ group in the films (40). The bands at 1,550 and 1,408 $cm^{-1}$ were assigned to the symmetric and anti-symmetric stretching of the $COO^-$ group (40,41). The broad peak around 1,550 $cm^{-1}$ was believed to be the overlapped peak of $COO^-$ and $NH_3^+$ peaks, because the $NH_3^+$ peak appears between 1,600 and 1,460 $cm^{-1}$ and in a complex between CH and poly(acrylic acid) the $NH_3^+$ peak

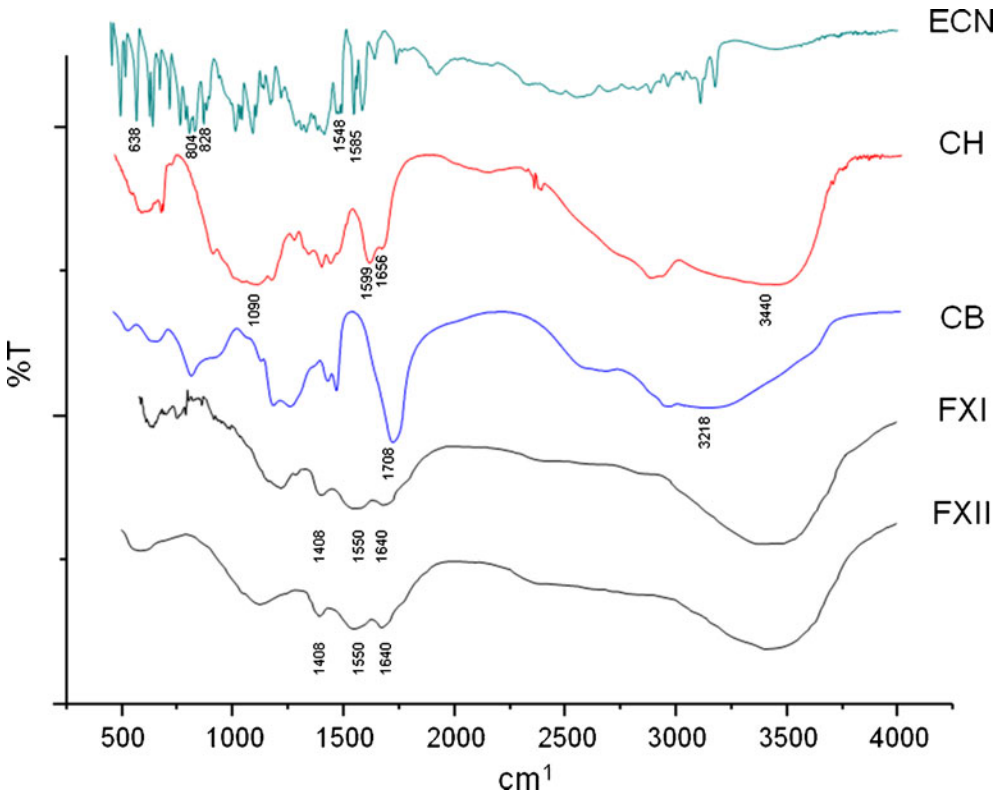


**Fig. 2.** FTIR spectra of pure ECN, CB and CH powders, and films *FXI* and *FXII*

appears at 1,520 $cm^{-1}$. These results suggest that the CH/CB film was formed by electrostatic interactions between the $COO^-$ group of CB and the $NH3^+$ group of CH (42). The spectrum of formulation FXII containing ECN was similar, and able to be overlapped to the formulation FXI without drug. This is an indication of absence of interactions between both polymers and ECN. This fact could be explained based on intermolecular interactions which may occur when two compounds are miscible. This will be reflected in changes of the infrared spectra of the mixture, such as wavenumber shifts, band broadening, and new absorption bans that are evidence of the compounds miscibility. Because the drug was dispersed as a solid form in the polymeric matrix during the film formulation, polymers and drug were immiscible and therefore it is expected that the resulting infrared spectrum will be the sum of the spectra of the individual compounds (43). Since the drug is only 1% of the formulation, characteristic peaks of ECN are very weak by a dilution effect.

### *Thermal Gravimetric Analysis and Differential Thermal Analysis*

The thermal stability and the degradation behavior of pure ECN, CB, and CH powders and CH films with and without ECN were studied by TGA-DTA under oxygen atmosphere. The TG and DTA curves of the samples are shown in Fig. 3. Figure 3a shows the TG curves of the starting materials: there was no weight loss until ECN melting (162–166°C), while the loss of ECN mass at 168°C could be attributed to the decomposition of drug after melt (44). The CH powder presents a characteristic chain degradation around 300°C and CB shows two peaks at 80°C (water evaporation) and at 250–350°C, referred to a thermal degradation at which CB melts and decomposes sequentially (45). In films containing 100% CH without drug, three steps of thermo-oxidative degradation were observed. The first one, in the temperature range 60–120°C, was attributed to the loss of absorbed water. The second one, at around 270°C, corresponds to the chemical degradation and deacetylation of chitosan (46). The third step, in the temperature range 450–600°C (data not shown), can be associated with the oxidative degradation of the carbonaceous residue formed during the second step. In films containing CB, the water loss was observed at 40–150°C and its degradation in the range 270–350°C. However, the mass loss process in the temperature range studied is much more gradual than the films containing 100% CH (FIV; Fig. 3b). When the results of CH/CB are compared with the results of CH in terms of the thermal behaviors, there are many important differences which might be due to the interaction between CH and CB. However, the characteristic peak of ENC appears unaltered in the films loaded with drug (Fig. 3c). This fact demonstrates that strong interactions between the matrix and the drug are absent.

### *Scanning Electron Microscopy*

SEM of polymers, drug and surfaces and cross-sections of the film membranes are shown in Fig. 4. The top views show the polymers and ECN. While CH blocks of around 100 μm present a smooth surface, CB and ECN appear as irregular crystals of different sizes. Formulations FIV, FVIII, and FXII show that all membranes are symmetric, uniformly distributed, and have a different morphology to wrinkles. It was also possible to observe that such wrinkles became much more evident on membranes with CB. Formulation FXII, which had 20% of CB, was the one in which a pattern of peaks and valleys

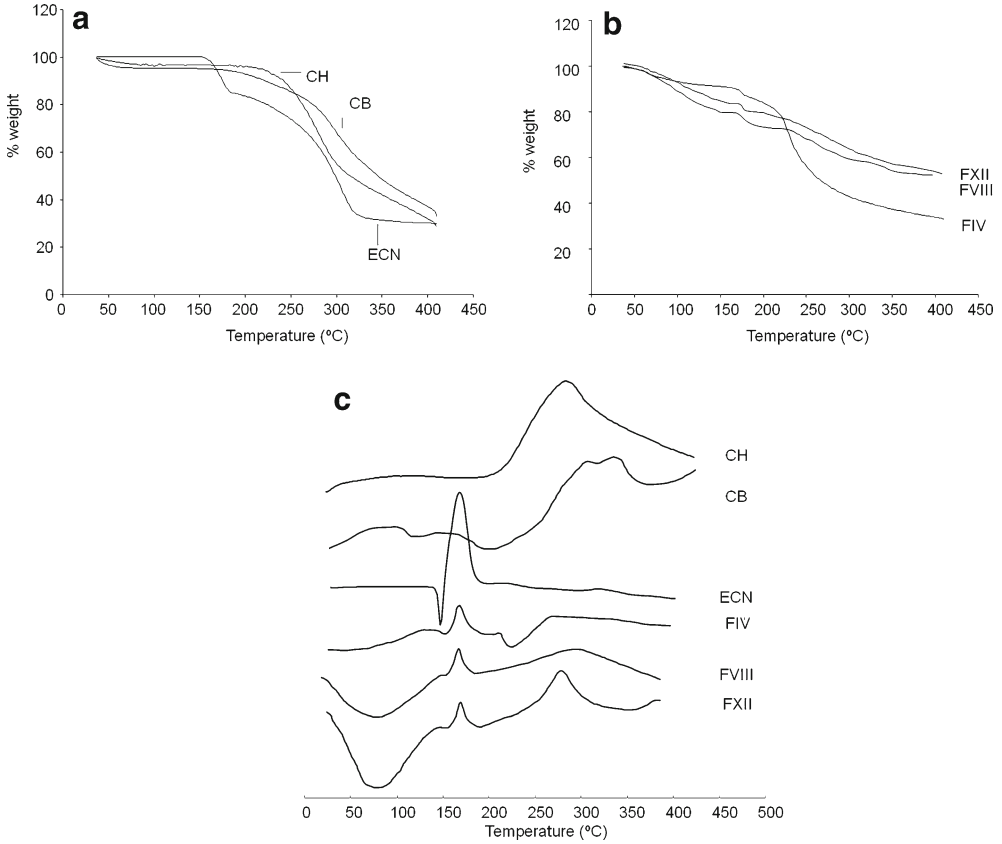


**Fig. 3.** Thermal stability and degradation behavior of pure ECN, CB, and CH powders and films loaded with ECN; **a** and **b** thermal analysis, **c** differential thermal analysis

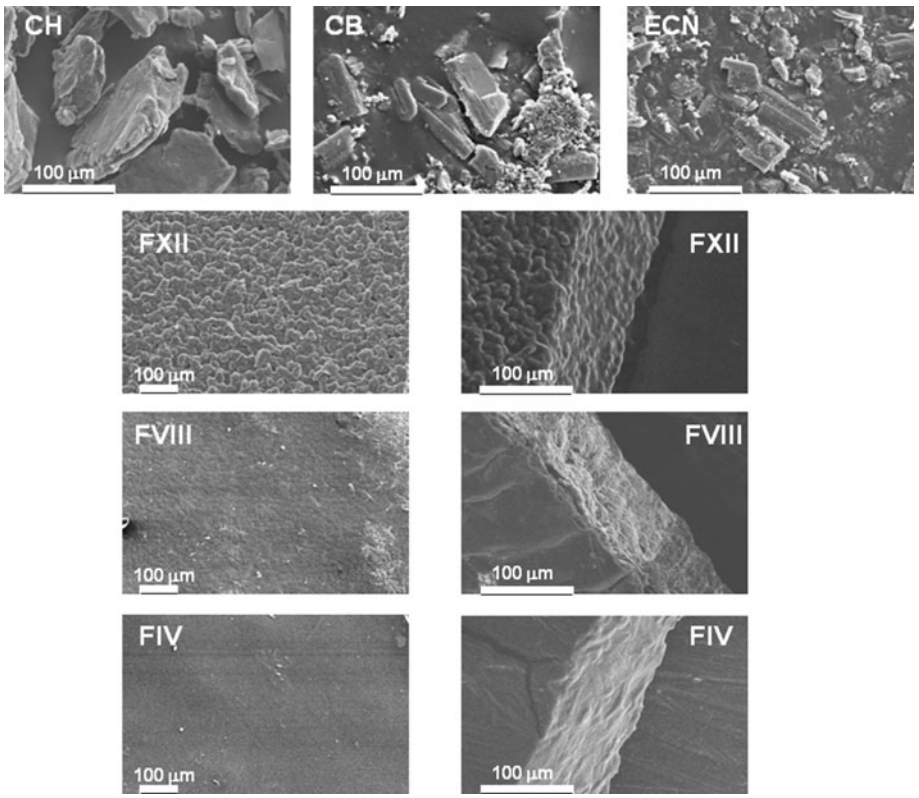


**Fig. 4.** Scanning electron microscopy of polymers (CH and CB), drug (ECN), and surfaces and cross-sections of films membranes containing ECN and different amount of CH and CB (FIV: CH 100%, CB 0%; FVIII: CH 90% CB 10%; and FXII: CH 80% CB 20%)

was more pronounced, probably due to the higher occurrence of interactions in this membrane because CB is present in higher concentration and is able to form a larger number of electrostatic interactions and hydrogen bonds with CH.

Small crystals (probably of drug) can be observed over the surface of the films, which could be another indication that no interaction between polymers and ECN occurs.

*Atomic Force Microscopy*

The AFM images of the different formulations and their rugosity distributions are shown in Fig. 5. As can be seen, 100% CH films show an almost plane structure, with a rugosity distribution around 500 nm. However, the peak and valley pattern observed by SEM was notorious in films with CB (formulations FVII, FVIII, FXI, and FXII). Such a pattern can be observed over an extensive area of the membrane surface, showing a distribution of rugosity around 1–1.3 μm for CB 10% and 2–3.5 μm for CB 20%. Additionally, the films loaded with ECN show incrustations (probably of drug) in the structure of the matrix, which increase slightly the dispersion of the rugosity. This peak and valley pattern is due to local variations on polymer concentration causing a change on interfacial tension and inducing additional convection at the interface (31,47).

*Water Uptake*

The water uptake profiles of the films are shown in Fig. 6. When the assay was carried out in a solution pH 7.2 (Fig. 6a), FIV (100% CH) reaches its maximum of water sorption at 120 min, after that time, reaches an equilibrium state and no lost of weight was observed during the assay. On the other hand, formulations FVIII (90% CH and 10% CB) and FXII (80% CH and 10% CB) reach the maximum water uptake at 60 min, after that, a diminished in the weigh by erosion of the matrix was observed. This result could be due to the films with CH and CB became more hydrophilic than CH alone, producing strong polar sites, generating better interactions between matrix and solvent and therefore producing faster water uptake (11,31). The loss of weight observed in formulation FVIII and FXII could be attributed to the partial solubilization of CB in the medium pH 7.2 generating the erosion of the film. When the water uptake was assayed in an acidic medium, the maximum water uptake was allowed at 60 min and the weight loss was evident in all three formulations. The mentioned effect was more pronounced in FIV (100% CH). This result may due to films are based on CH and this polymer is soluble in acidic medium (Fig. 6b).

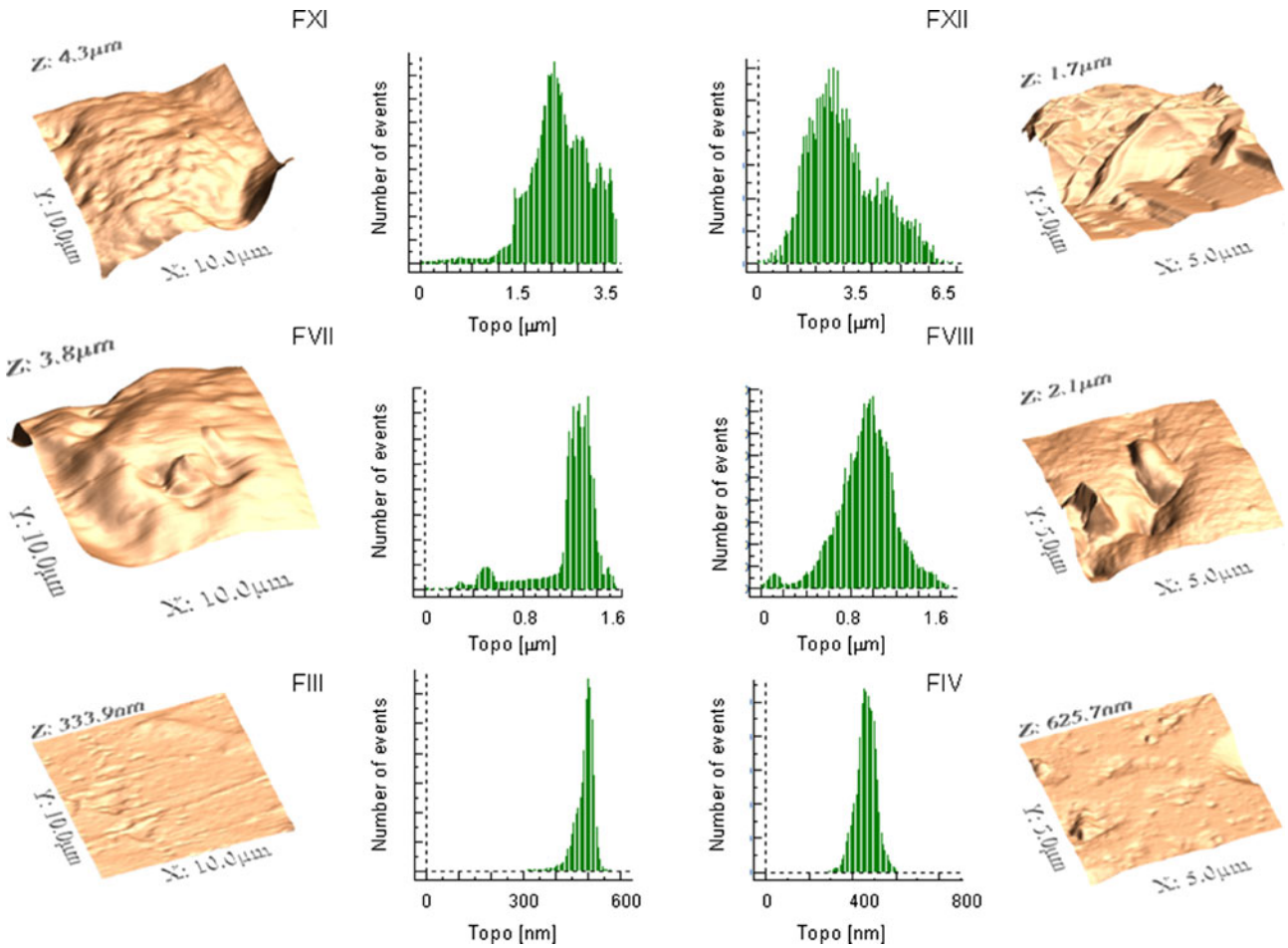


**Fig. 5.** Atomic force microscopy of surfaces films membranes with different content of CH and CB with ECN 1% (FIV: CH 100% CB 0%; FVIII: CH 90% CB 10%; FXII: CH 80% CB 20%) and without ECN (FIII: CH 100% CB 0%; FVII: CH 90% CB 10%; FXI: CH 80% CB 20%)

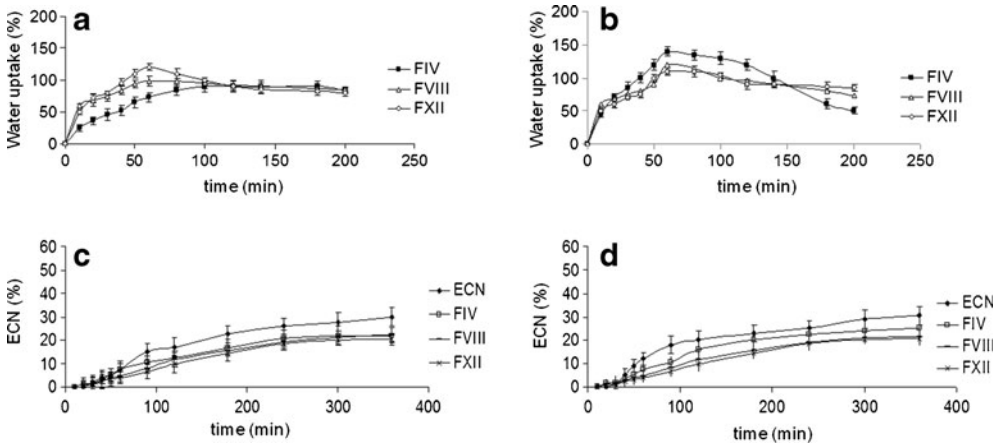


**Fig. 6.** Water uptake (**a** and **b**) and dissolution profiles (**c** and **d**) of films containing ECN and different amount of CH and CB; **a** and **c** pH 7.2, **b** and **d** pH 4.2

*Dissolution Assay*

To obtain a complete characterization of the systems, the release of ECN from FIV, FVIII, and FXII was evaluated at two pH values (Fig. 6c, d). Although ECN is a poorly water-soluble drug (48), it was solubilized faster than the drug loaded into the films, but, independently of the pH value, the ECN dissolution profile was not significantly modified. When a water-soluble drug is loaded into a CH matrix, there is an initial burst effect in the early stage of the dissolution; this fact is due to the disintegrative effect of the hydrophilic drug which takes water rapidly by capillarity through available pores in the matrix (49). After this initial hydration of the films, gel formation of chitosan ($p$K$_a$ 6.5) in acid buffer medium (pH 4.2) causes clogging of pores and thus hindering the entrance of water. Therefore, drug is released from the films by slow diffusion through the gel layer (50). However and due to ECN is a hydrophobic poorly water-soluble drug, no significant differences were observed between the dissolution profiles at different pH values. After 6 h assay just 30% of ECN was solubilized; this value is in good agreement with the one found in the literature (51). Based on the obtained dissolution profiles and in the results of water uptake assay, the release of the drug from this polymeric matrix may be due to diffusion at the beginning of the assay and then by a combination of diffusion and erosion.

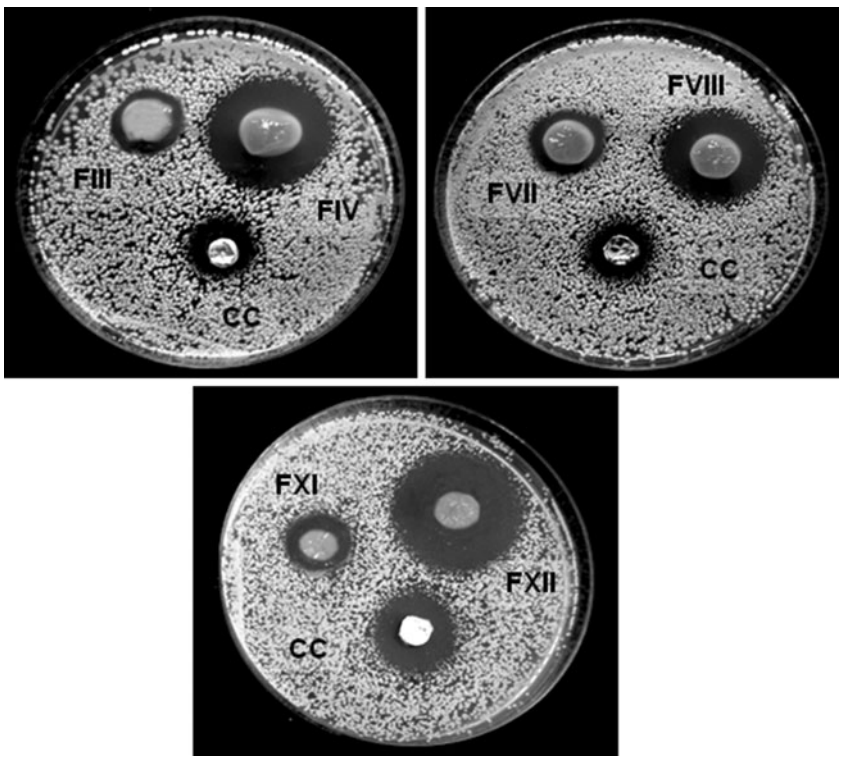


**Fig. 7.** Halos of growth inhibition produced by films without ECN (*FIII*, *FVII*, *FXI*) and loaded with ECN (*FIV*, *FVIII*, *FXII*) and a commercial cream (*CC*) in a culture of *Candida krusei*

*Halo Zone Test*

Due to its importance in connection with the release and activity of the drug loaded in the polymeric matrix, an antifungal assay for the films was developed. Films without drug, and a commercial cream containing the same content of ECN were designed as controls. After a 24-h assay, the growth inhibition of *C. krusei* was shown as dark areas around the films (Fig. 7).

Similar areas were obtained for *C. parapsilosis*, indicating no significant differences between the yeasts ($p > 0.05$). As can be observed, the three formulations assayed produced similar 100% inhibition hales (9.0±1.0 mm) and significant differences ($p < 0.05$) with respect to the controls (6.5±0.5 mm). Films without drug also showed an inhibition zone (6.0±0.5 mm) that could be explained by the previously reported antimicrobial activity of CH (52–59), which generates a matrix with antifungal properties. Surprisingly, the halo zone of the commercial cream (CC) containing an amount of ENC equal to that in the films was half in diameter for the both yeast assayed. This fact may probably be the result of the sum of the antifungal activity of ECN and the "environmental and eco-friendly" matrix. Therefore, it will be possible to produce a new pharmaceutical form based on a polymeric film containing ECN, which could be loaded with a small drug concentration, and however produce the same therapeutic effect against *C. krusei* and *C. parapsilosis.*

*Stability Study*

Stability studies carried out for formulations FIV, FVIII, and FXII at 25°C, or 40°C and 58% RH revealed no significant differences in drug content after a year. Mean drug content for 1 year was above 98% at 25°C, and above 95% at 40°C.

## CONCLUSIONS

In this work, several formulations containing CH, CB, and ECN were developed and studied. The application of CH–CB films to load and release an antifungal drug was demonstrated. The IR and ATD-TG analysis showed interactions between the polymers. By SEM and AFM, drug crystals over the films surface were observed. The rugosity distribution of the systems was associated to the interactions between polymers. The matrix was able to release the drug in both neutral and acid medium probably by a combination between drug diffusion and matrix erosion. The *in vitro* antifungal activity was assayed against *C. krusei* and *C parapsilosis*, showing the sum of antifungal effects of ECN and CH, producing larger inhibition halos than the same ECN concentration in a commercial cream. Finally, formulations FIV, FVIII, and FXII containing S as plasticizer and 1% ECN showed good mechanical properties and good antifungal activity. These formulations are potential candidates for the development of alternatives pharmaceutical form for the treatment of *Candida*, based on the activity of the eco-friendly matrix added to the econazole nitrate activity.

## ACKNOWLEDGMENTS

The National University of Rosario (UNR), the National Council Research (CONICET, Argentina), and ANPCyT (Agencia Nacional de Promoción Científica y Tecnológica) are gratefully acknowledged for financial support.

## REFERENCES

1. Pillai CKS, Paul W, Sharma CP. Chitin and chitosan polymers: chemistry, solubility and fiber formation. Prog Polym Sci. 2009;34:641–78.
2. Ziani K, Ursúa B, Maté JI. Application of bioactive coatings based on chitosan for artichoke seed protection. Crop Prot. 2010;29:853–9.
3. Smitha B, Sridhar S, Khan A. Chitosan-sodium alginate polyion complexes as fuel cell membranes. Eur Polym J. 2005;41:1859–66.
4. Yan X, Khor E, Lim LY. PEC films prepared from chitosan-alginate coacervates. Chem Pharm Bull. 2000;48:941–6.
5. Ma L, Gaoa C, Mao Z, Zhou J, Shen J, Hu X, Han C. Collagen/chitosan porous scaffolds with improved biostability for skin tissue engineering. Biomaterials. 2003;24:4833–41.
6. Majeti NV, Ravi K. A review of chitin and chitosan applications. React Funct Polym. 2000;46:1–27.
7. Shi CH, Shieh YT, Twu YK. Preparation and characterization of cellulose/chitosan films. Carbohydr Polym. 2009;78:169–74.
8. Vargas M, Albors A, Chiralt A, Gonzalez-Martinez C. Characterization of chitosan-oleic acid composite films. Food Hydrocoll. 2009;23:536–47.
9. Portes E, Gardrat C, Castellan A, Coma V. Environmentally friendly films based on chitosan and tetrahydrocurcuminoid derivatives exhibiting antibacterial and antioxidative properties. Carbohydr Polym. 2009;76:578–84.
10. Mura P, Corti G, Cirri M, Maestrelli F, Mennini N, Bragagni M. Development of mucoadhesive films for buccal administration of flufenamic acid: effect of cyclodextrin complexation. J Pharm Sci. 2010;99:3019–29.
11. de la Torre PM, Enobakhare Y, Torrado G, Torrado S. Release of amoxicillin from polyionic complexes of chitosan and poly(acrylic acid). Study of polymer/polymer and polymer/drug interactions within the network structure. Biomaterials. 2003;24:1499–506.
12. Perioli L, Ambrogi V, Pagano C, Scuota S, Rossi C. FG90 chitosan as a new polymer for metronidazole mucoadhesive tablets for vaginal administration. Int J Pharm. 2009;377:120–7.
13. Silva CL, Pereira JC, Ramalho A, Pais AACC, Sousa JJS. Films based on chitosan polyelectrolyte complexes for skin drug delivery: development and characterization. J Membr Sci. 2008;320:268–79.
14. Nitayaphat W, Jiratumnukul N, Charuchinda S, Kittinaovarat S. Mechanical properties of chitosan/bamboo charcoal composite films made with normal and surface oxidized charcoal. Carbohydr Polym. 2009;78:444–8.
15. Dobrynin AV, Rubinstein M. Theory of polyelectrolytes in solutions and at surfaces. Prog Polym Sci. 2005;30:1049–118.
16. Barreiro-Iglesias R, Alvarez-Lorenzo C, Concheiro A. Incorporation of small quantities of surfactants as a way to improve the rheological and diffusional behavior of carbopol gels. J Control Release. 2001;77:59–75.
17. Zipfel PF, Skerkaa C, Kupkaa D, Luoa S. Immune escape of the human facultative pathogenic yeast *Candida albicans*: the many faces of the Candida Pra1 protein. Int J Med Microbiol. 2011;301:423–30.
18. Monk B, Goffeau A. Outwitting multidrug resistance to antifungals. Science. 2008;321:367–9.
19. Hof H. Mykologie fur mediziner. Stuttgart: Thieme-Verlag; 2003.
20. Weitzman I, Summerbell R. The dermatophytes. Clin Microbiol Rev. 1995;8:240–59.
21. Seyfarth F, Schliemann S, Elsner P, Hipler UC. Antifungal effect of high- and low-molecular-weight chitosan hydrochloride, carboxymethyl chitosan, chitosan oligosaccharide and *N*-acetyl-D-glucosamine against *Candida albicans*, *Candida krusei* and *Candida glabrata*. Int J Pharm. 2008;353:139–48.

22. Albertini B, Passerini N, Di Sabatino M, Vitali B, Brigidi P, Rodriguez L. Polymer–lipid based mucoadhesive microspheres prepared by spray-congealing for the vaginal delivery of econazole nitrate. Eur J Pharm Sci. 2009;36:591–601.
23. Dyas AM, Delargy H. Econazole nitrate. In: Florey K, editor. Analytical profiles of drug substances, 23. New York: Academic Press; 1994. p. 125–51.
24. Acartürk F. Mucoadhesive vaginal drug delivery systems. Recent Pat Drug Deliv Formul. 2009;3:193–205.
25. Gavini E, Sanna V, Julianno C, Bonferoni MC, Giunchedi P. Mucoadhesive vaginal tablets as veterinary delivery system for the controlled release of an antimicrobial drug, acriflavine. AAPS PharmSciTech. 2002;3(3):article 20.
26. Valenta C. The use of mucoadhesive polymers in vaginal delivery. Adv Drug Deliv Rev. 2005;57(11):1692–712.
27. Lehr CM, Bouwstra JA, Schacht EH, Junginger HE. *In vitro* evaluation of mucoadhesive properties of chitosan and some other natural polymers. Int J Pharm. 1992;78:43–8.
28. Khan TA, Peh KK, Chang HS. Mechanical, bioadhesive strength and biological evaluation of chitosan films for wound dressing. J Pharm Pharm Sci. 2000;3:303–11.
29. Berger J, Reist M, Mayer JM, Felt O, Gurny R. Structure and interactions in chitosan hydrogels formed by complexation or aggregation for biomedical applications. Eur J Pharm Biopharm. 2004;57(1):35–52.
30. Cardenas G, Miranda P. FTIR and TGA studies of chitosan composite films. J Chil Chem Soc. 2004;49(4):291–5.
31. de Oliveira HC, Fonseca JL, Pereira MR. Chitosan-poly(acrylic acid) polyelectrolyte complex membranes: preparation, characterization and permeability studies. J Biomater Sci Polym. 2008;19(2):143–60.
32. Chen CH, Lai LS. Mechanical and water vapor barrier properties of tapioca starch decolorized hsian-tsao leaf gum films in the presence of plasticizer. Food Hydrocoll. 2008;22:1584–95.
33. Shellhammer TH, Krochta JM. Whey protein emulsion film performance as affected by lipid type and amount. J Food Sci. 1997;62:390–4.
34. Horcas I, Fernández R, Gómez-Rodríguez JM, Colchero J, Gómez-Herrero J. WSXM: a software for scanning probe microscopy and a tool for nanotechnology. Rev Sci Instrum. 2007;78:013705. doi:10.1063/1.2432410.
35. Lee TW, Kim JC, Hwang SJ. Hydrogel patches containing triclosan for acne treatment. Eur J Pharm Biopharm. 2003;56(3):407–12.
36. Leonardi D, Barrera MG, Lamas MC, Salomon CJ. Development of prednisone:polyethylene glycol 6000 fast-release tablets from solid dispersions: solid-state characterization, dissolution behavior, and formulation parameters. AAPS PharmSciTech. 2007;8(4):221–8.
37. Domjan A, Bajdik J, Pintye-Hodi K. Understanding of the plasticizing effects of glycerol and PEG 400 on chitosan films using solid-state NMR spectroscopy. Macromolecules. 2009;42:4667–73.
38. Al-Marzouqi AH, Elwy HM, Shehadi I, Adem A. Physicochemical properties of antifungal drug-cyclodextrin complexes prepared by supercritical carbon dioxide and by conventional techniques. J Pharm Biomed Anal. 2009;49:227–33.
39. Vasconcellos FC, Goulart GAS, Beppu MM. Production and characterization of chitosan microparticles containing papain for controlled release applications. Powder Technol. 2011;205:65–70.
40. de la Torre PM, Torrado S, Torrado S. Interpolymer complexes of poly(acrylic acid) and chitosan: influence of the ionic hydrogel-forming medium. Biomaterials. 2003;24:1459–68.
41. Nunthanid J, Laungtna-anan M, Sriamornsak P, Limmatvaprirat S, Puttipipatkhachorn S, Lim LY, Khor E. Characterization of chitosan acetate as a binder for sustained release tablet. J Control Release. 2004;99:15–26.
42. Park SH, Chun MK, Choi HK. Preparation of an extended-release matrix tablet using chitosan/carbopol interpolymer complex. Int J Pharm. 2008;347:39–44.
43. Stuart B. Infrarred spectroscopy: fundamentals and applications. West Sussex: Wiley; 2004.
44. Oyler AR, Naldi RE, Facchine KL, Burinsky DJ, Cozine MH, Dunphy R, *et al*. Characterization of autoxidation products of the antifungal compounds econazole nitrate and miconazole nitrate. Tetrahedron. 1991;47(33):6549–60.
45. Gomez-Carracedo A, Alvarez-Lorenzo C, Gomez-Amoza JL, Concheiro A. Glass transitions and viscoelastic properties of Carbopol® and Noveon® compacts. Int J Pharm. 2004;274:233–43.
46. Wang SF, Shen L, Tong YJ, Chen L, Phang LY, Lim PQ, *et al*. Biopolymer chitosan/montmorillonite nanocomposites: preparation and characterization. Polym Degrad Stab. 2005;90:123–31.
47. Torres MA, Aimoli CG, Beppu MM, Frejlich J. Chitosan membrane with patterned surface obtained through solution drying. Colloids Surf A Physicochem Eng Asp. 2005;268:175–9.
48. Pedersen M, Bjerregaard S, Jacobsen J, Rommelmayer Larsen A, Mehlsen Sorensen A. An econazole β-cyclodextrin inclusion complex: an unusual dissolution rate, supersaturation, and biological efficacy example. Int J Pharm. 1998;165(1):57–68.
49. Nogami H, Nagai T, Fukuoka E, Sonobe T. Disintegration of the aspirin tablets containing potato starch and microcrystalline cellulose in various concentrations. Chem Pharm Bull. 1969;17:1450–5.
50. Miyazaki S, Yamaguchi H, Yokouchi C, Takada M, Hou WM. Sustained release of indomethacin from chitosan granules in beagle dogs. J Pharm Pharmacol. 1988;40:642–3.
51. Albertini B, Passerini N, Di Sabatino M, Vitali B, Brigidi P, Rodriguez L. Polymer–lipid based mucoadhesive microspheres prepared by spray-congealing for the vaginal delivery of econazole nitrate. Eur J Pharm Sci. 2009;36(4–5):591–601.
52. Palmeira de Oliveira A, Ribeiro MP, Palmeira de Oliveira R, Gaspar C, Costa de Oliveira S, Correia IC, *et al*. Anti-*Candida* activity of a chitosan hydrogel: mechanism of action and cytotoxicity profile. Gynecol Obstet Invest. 2010;70(4):322–7.
53. Chung YC, Su YP, Chen CC, Jia G, Wang HL, Wu JC, *et al*. Relationship between antibacterial activity of chitosan and surface characteristics of cell wall. Acta Pharmacol Sin. 2004;25:932–6.
54. Gil G, del Monaco S, Cerrutti P, Galvagno M. Selective antimicrobial activity of chitosan on beer spoilage bacteria and brewing yeasts. Biotechnol Lett. 2004;26:569–74.
55. Limam Z, Selmi S, Sadok S, El Abed A. Extraction and characterization of chitin and chitosan from crustacean by-products: biological and physicochemical properties. Afr J Biotechnol. 2011;10:640–7.
56. Tayel AA, Moussa S, El-Tras WF, Knittel D, Opwis K, Schollmeyer E. Anticandidal action of fungal chitosan against *Candida albicans*. Int J Biol Macromol. 2010;47:454–7.
57. Tikhonov VE, Stepnova EA, Babak VG, Yamskov IA, Palma-Guerrero J, Hans-Börje J, *et al*. Bactericidal and antifungal activities of a low molecular weight chitosan and its N-/2(3)-(dodec-2-enyl) succinoyl/-derivatives. Carbohydr Polym. 2006;64:66–72.
58. Wang X, Du Y, Yang J, Wang X, Shi X, Hu Y. Preparation, characterization and antimicrobial activity of chitosan/layered silicate nanocomposites. Polymer. 2006;47:6738–44.
59. Martínez-Camacho AP, Cortez-Rochaa MO, Ezquerra-Brauer JM, Graciano-Verdugo AZ, Rodriguez-Félix F, Castillo-Ortega MM, *et al*. Chitosan composite films: thermal, structural, mechanical and antifungal properties. Carbohydr Polym. 2010;82:305–15.